University of Lethbridge

HAMEL GROUP
organofluorine chemistry

# Decarboxylative functionalization of bicyclo[1.1.1]pentanes

**Honours Thesis**

**By: Christy Bore**

**Supervisor: Dr. Jean-Denys Hamel**

**Second Reader: Dr. Greg Patenaude**

**Fall 2023 – Spring 2024**

# Table of Contents

# List of Schemes

# List of Figures

# List of Abbreviations

| | |
|---|---|
| acac | acetylacetone |
| aq. | aqueous |
| $B_2Cat_2$ | bis(catecholato)diboron |
| $B_2Pin_2$ | bis(pinacolato)diboron |
| BCP | bicyclo[1.1.1]pentan-1-yl |
| cat. | catalytic |
| DCM | dichloromethane |
| DIC | *N,N'*-diisopropylcarbodiimide |
| DMAP | 4-(*N,N*-dimethylamino)pyridine |
| DMF | *N,N'*-dimethylformamide |
| dtbbpy | 4,4′-bis(1,1-dimethylethyl)-2,2′-bipyridine |
| Eq | equivalent |
| glyme | ethylene glycol dimethyl ether |
| $K_i$ | inhibitory constant |
| LED | light-emitting diode |
| Me | methyl |
| MeObipy | 4-4′-dimethoxy-2-2′-bipyridine |
| min | minute |
| NHPI | *N*-hydroxyphthalimide |
| NHS | *N*-hydroxysuccinimide |
| NMR | nuclear magnetic resonance |
| Ph | phenyl |
| Nphth | phthalimide |
| p$K_a$ | negative logarithm of acid dissociation constant |
| ppy | phenylpyridinato |
| RAE | redox-active ester |
| RT | room temperature |

| | |
|---|---|
| Selectfluor | 1-chloromethyl-4-fluoro-1,4-diazoniabicyclo[2.2.2]octane bis(tetrafluoroborate) |
| SET | single-electron transfer |
| TCNHPI | *N*-hydroxytetrachlorophthalimide |
| THF | tetrahydrofuran |

# 1. Introduction

## 1.1 Introduction to organofluorine chemistry

Organofluorine chemistry involves organic compounds containing C–F bonds. Fluorinated organic compounds have been shown to have applications in many different fields including medicinal chemistry, agrochemicals, and materials chemistry.[1-3] The interest in organofluorine chemistry comes from the unique properties that fluorine can impart, part of which is due to strength of the C–F bond, which is the strongest single bond in organic chemistry at 105.4 kcal/mol (**Table 1**).[4, 5] The strength of the C–F bond, which is stronger than the C–H bond which is considered to be inert, can help to improve metabolic stability of compounds as the C–F bond is more resistant to metabolic attack than other common bonds found in organic molecules.[3]

*Table 1: Bond dissociation energy for common covalent bonds in organofluorine chemistry.*[5]

| **Bond** | **Bond Dissociation Energy (kcal/mol)** |
|---|---|
| C–F | 105.4 |
| C–H | 98.8 |
| C–O | 84.0 |
| C–C | 83.1 |
| C–Cl | 78.5 |
| C–N | 69.7 |

Fluorine may also improve metabolic stability of compounds due to electrostatic effects, as well as resonance/inductive effects.[6] Fluorine is the most electronegative atom, with an electronegativity of 3.98 on the Pauling scale.[3] Due to its high electronegativity, it is able to alter electron distribution which can impact the p$K_a$, dipole moment, and the stability and chemical reactivity of neighbouring functional groups.[6] Fluorine may also improve binding affinity of compounds by direct interactions with target proteins, or indirectly by influencing the polarity of other groups present on the compound.[6]

An example compound that can be used to show the effects of fluorine is Atogepant, which is a medication commonly used for migraines.[7] When comparing Atogepant to Ubrogepant, its unsubstituted derivative (**Figure 1**), Atogepant has a higher affinity ($K_i$ = 0.015 nM) than Ubrogepant ($K_i$ = 0.067 nM).[3, 8] Indeed, with $K_i$ being the inhibitory constant, which represents the concentration of drugs required to occupy 50% of receptors, the lower the $K_i$ the stronger the binding affinity to the receptors.[9]

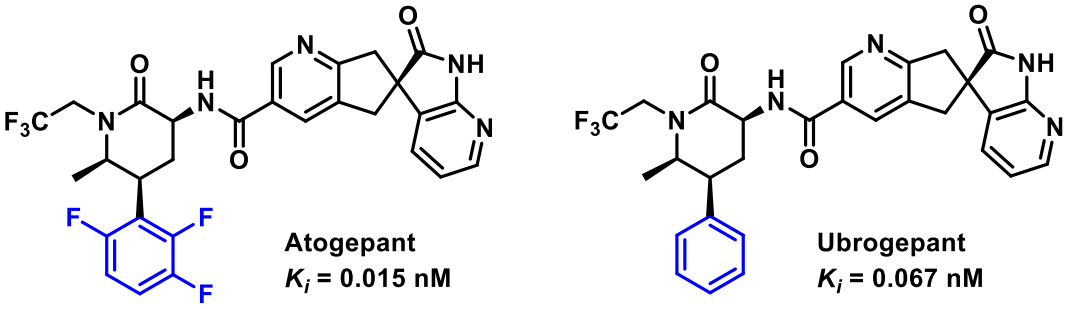


*Figure 1: Atogepant and its non-trifluoroaryl derivative Ubrogepant, and their inhibitory constants.*

Growing interest in compounds containing C–F bonds, has led to a surge in the development of new organofluorine compounds. Previous methods to synthesize organofluorine compounds in the 1960s and 1970s typically involved the use of gaseous fluorine, or other compounds such as perchloryl fluoride or xenon difluoride which are electrophilic fluorinating sources (**Figure 2**).[10]

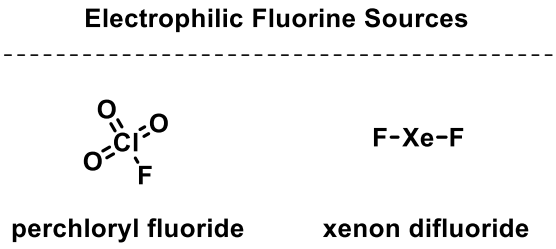


*Figure 2: Electrophilic fluorine sources previously used in the synthesis of fluorinated compounds.[10]*

Due to the demand for fluorinated compounds and the aggressive nature of the previously used reagents, with perchloryl fluoride being explosive, and xenon difluoride known to react with moisture to form hydrofluoric acid, there has been studies done to discover safer and greener ways to prepare fluorinated compounds, most commonly which involve the use of fluorinating agents that have nucleophilic character (ex. DAST), or electrophilic and/or radical character (ex. Selectfluor and NFSI) (**Figure 3**).[10]

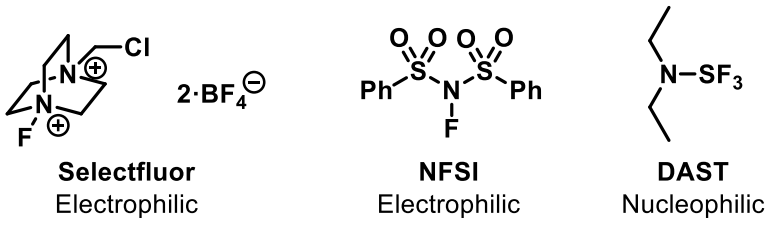


*Figure 3: Structure of common fluorinating agents and their fluorinating character.*[10]

## 1.2 Introduction to bioisosteres of benzene rings

Benzene rings have a long history of use in organic chemistry and drug design, with phenyl rings being a component of around 45% of marketed small molecule drugs, and their prevalence being 10 times higher than the second most popular ring, pyridine, in drug design.[11] Part of this is due to the diversity of substituents that can be added to phenyl rings, the ease in which phenyl rings can be introduced, and its role as a scaffolding element that allow the projection of substituents along well-defined exit vectors.[11] Introspective analyses of medicinal chemistry practices at the beginning of the 21st century have determined that there has been an overuse of phenyl rings and other aromatic units in drug design, which has led to poor physiochemical properties of molecules, thereby limiting their prospects of being developed into effective drugs.[11] Part of the issues with phenyl rings in drug design comes from the structure's planarity. Past research has shown that "escaping from Flatland" by exchanging $sp^2$-hybridized carbons for $sp^3$-hybridized carbons can result in compounds that access a chemical space that is relatively untested, and increases the chance that the compound will be bioavailable and bioactive.[12] Bioavailability is the extent and rate at which bioactive drug compounds are absorbed and available at the site of action.[13] With the recent understanding of the potential negative impacts of the overuse of phenyl rings, there has been a desire to discover bioisosteres of phenyl rings. Bioisosteres are compounds or groups that

have similar molecular shapes and produce similar biological properties.[14] One of these potential bioisosteres for phenyl rings is bicyclo[1.1.1]pentanes (BCPs) (**Figure 4**).


*Figure 4: Structure of BCP with R groups at its bridgehead positions.*

Though BCPs were first synthesized in 1964 by Wiberg and coworkers,[15] they were for the most part ignored until 2012 when interest in the field of BCPs began with Stepan and colleagues at Pfizer synthesizing a BCP analogue of avagacestat, a drug used to treat Alzheimer's disease (**Figure 5**).[16, 17] Analogue **B** was shown to exhibit equivalent biological activity to **A**, in addition to enhanced solubility, membrane permeability, and reduced metabolic susceptibility. [16]

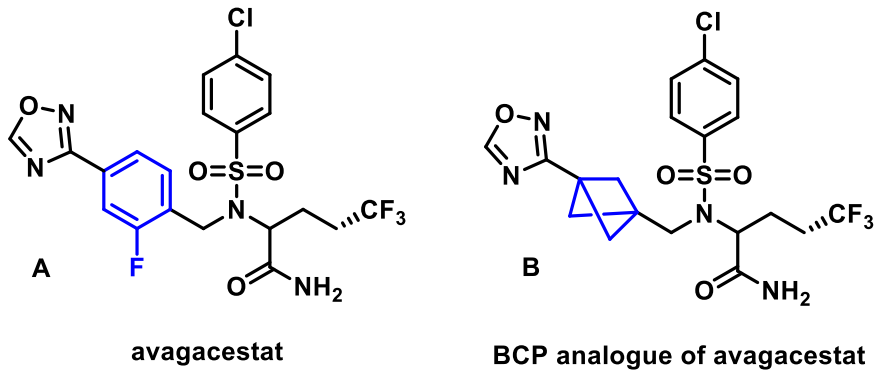


*Figure 5: Structure of avagacestat (A) and its BCP analogue (B).*

BCPs can serve as an $sp^3$-rich scaffold that is able to mimic the geometry and substituent exit vectors of a phenyl ring, while also offering similar biological properties of phenyl rings.[16] The bridgehead substituents of a BCP have the same 180° exit vector of *para*-substituted arenes with an approximate 1.1 Å decrease in distance between key carbon atoms bearing the substituents (**Figure 6**).

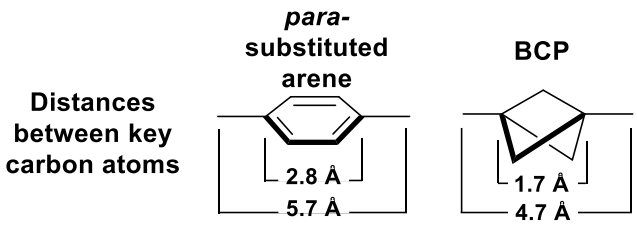


*Figure 6: Image showcasing the 180° angles of para-substituted arenes and a BCP, as well as distances between key carbon atoms.*

Since the report of Stepan and colleagues in 2012, 250 research papers have been published involving BCPs as of 2022.[18] Of the 250 papers published, many have shown that the exchange of a phenyl group for a BCP tends to improve pharmacological properties; however, that was not always the case with some papers reporting that the exchange of the phenyl group for a BCP led to decreased bioactivity, potentially due to the loss of the π-π interactions normally attributed to the phenyl ring.[16] The majority of the papers underlined the relatively consistent ability of BCPs to increase the solubility of the drug compounds, with other properties such as metabolic stability, potency, and bioactivity being less easy to predict.

With our interest in fluorine and the remarkable properties it can important to compounds, as well as BCPs and their function as a bioisosteres for phenyl rings, our focus was placed on fluorinated BCPs and how we might synthesize them and install them onto compounds.

## 1.3 Redox-active esters

One method hypothesized for the installation of these fluorinated BCPs would be through coupling reactions that focused on the use of redox-active esters (RAE). Redox-active esters (RAE) are compounds that have an inclination towards single-electron reduction, and are often derived from *N*-hydroxyphthalimide (NHPI), *N*-hydroxytetrachlorophthalimide (TCNHPI), and *N*-hydroxysuccinimide (NHS) (**Figure 7**).[19] These compounds have a history of being easy to prepare, being highly stable under most conditions, and serving as radical precursors as they are able to undergo reductive decarboxylation to provide a radical intermediate able to engage in a diverse range of transformations.[19]

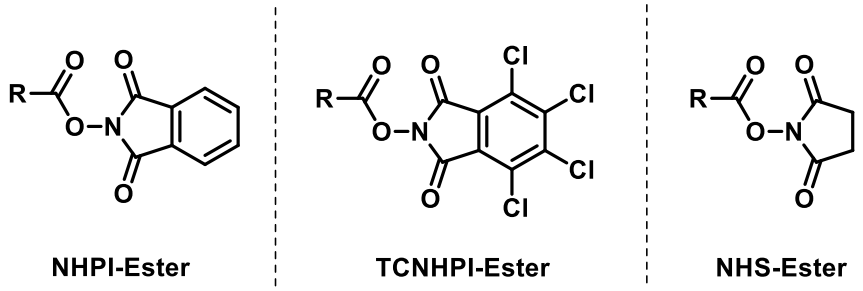


*Figure 7: Structures of NHPI-ester, TCHNPI-ester and NHS-ester used in this study.*

These redox-active esters have been shown in literature to be able to undergo reductive decarboxylation to form C(*sp*$^3$) radicals.[19, 20] Assuming that a carboxylic acid is available, the first step involves the esterification of carboxylic acid to form the RAE, and then SET followed by fragmentation to form carbon dioxide, a C(*sp*$^3$) radical and a cyclic imide anion (**Scheme 1**).

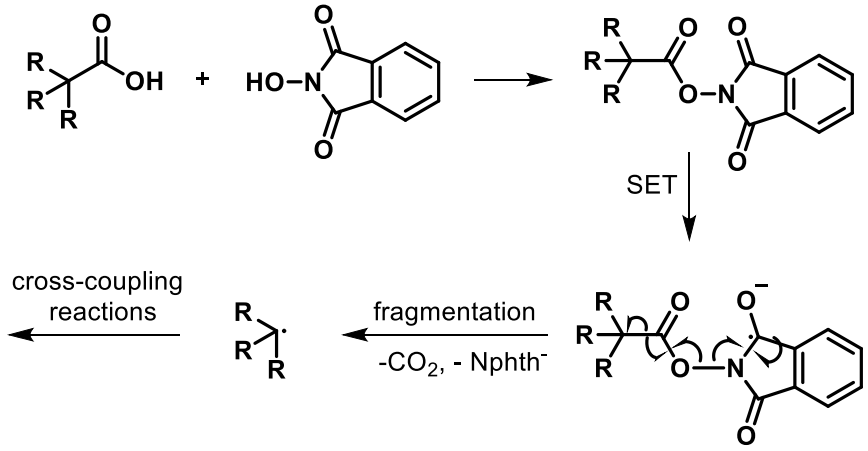


*Scheme 1: General pathway for reductive decarboxylative reactions of NHPI esters, starting from a carboxylic acid.*

With literature indicating RAEs to be good starting materials to form C(*sp*$^3$) radicals and our desired radicals to be of the BCP, which contain *sp*$^3$-hybridized carbons, RAEs were chosen as the primary starting material of study.

# 2. Previous Research

## 2.1 Preparation of F-BCP-Acid and F-BCP-NHPI

Work has been done by me and another student (Stacie Nelson) in previous semesters to prepare RAE containing a fluorinated BCP, which will be referred to from this point as F-BCP-NHPI and other RAE analogues. There were some challenges that were overcome, first with the preparation of the F-BCP-Acid (**2**) compound by decarboxylative fluorination of bicyclo[1.1.1]pentane-1,3-dicarboxylic acid (**1**) (**Scheme 2**).

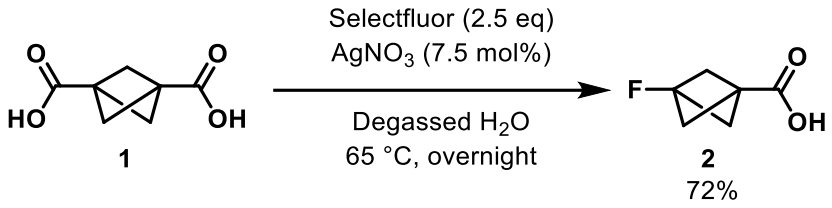


*Scheme 2: Decarboxylative fluorination of dicarboxylic acid (**1**).*

First attempts to synthesize this product were met with low yields, which were later determined to be caused by sublimation, as well as old starting material. Once new starting material had been purchased and special care was placed on preventing the product from being under vacuum for long periods of time, the yield was increased from around 13% to 72%.

The synthesized F-BCP-Acid (**2**) was then used in a Steglich esterification reaction in which the F-BCP-Acid is reacted with NHPI, in the presence of DIC as a coupling agent, and DMAP as a nucleophilic catalyst to form F-BCP-NHPI (**3**).[21] Synthesis of **3** caused no issues and was easily isolated with high yield using silica gel chromatography.

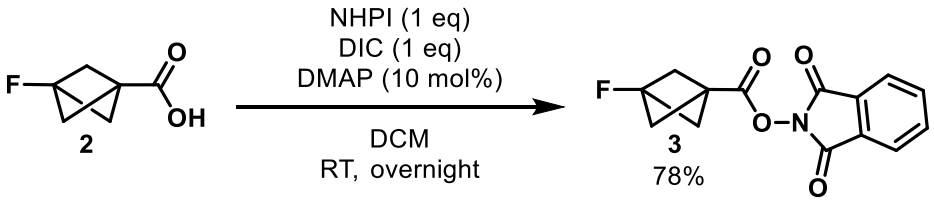


*Scheme 3: Steglich esterification of F-BCP-Acid **2** with NHPI.*

With the successful formation of the desired RAE, attempts were then made to use the prepared compound in reductive decarboxylative reactions, the first of which was to form a boron species that could be used in cross-coupling reactions like the Suzuki-Miyaura reaction.[22]

## 2.2 Borylation reactions with F-BCP-NHPI

Three different literature papers were followed to attempt to form F-BCP-Bpin (**4**) that would subsequently be used in Suzuki-Miyaura cross-coupling reactions (**Scheme 4**).[21, 23, 24] All attempts were met with either no yield or very low yield of products that were unable to be isolated using purification techniques.

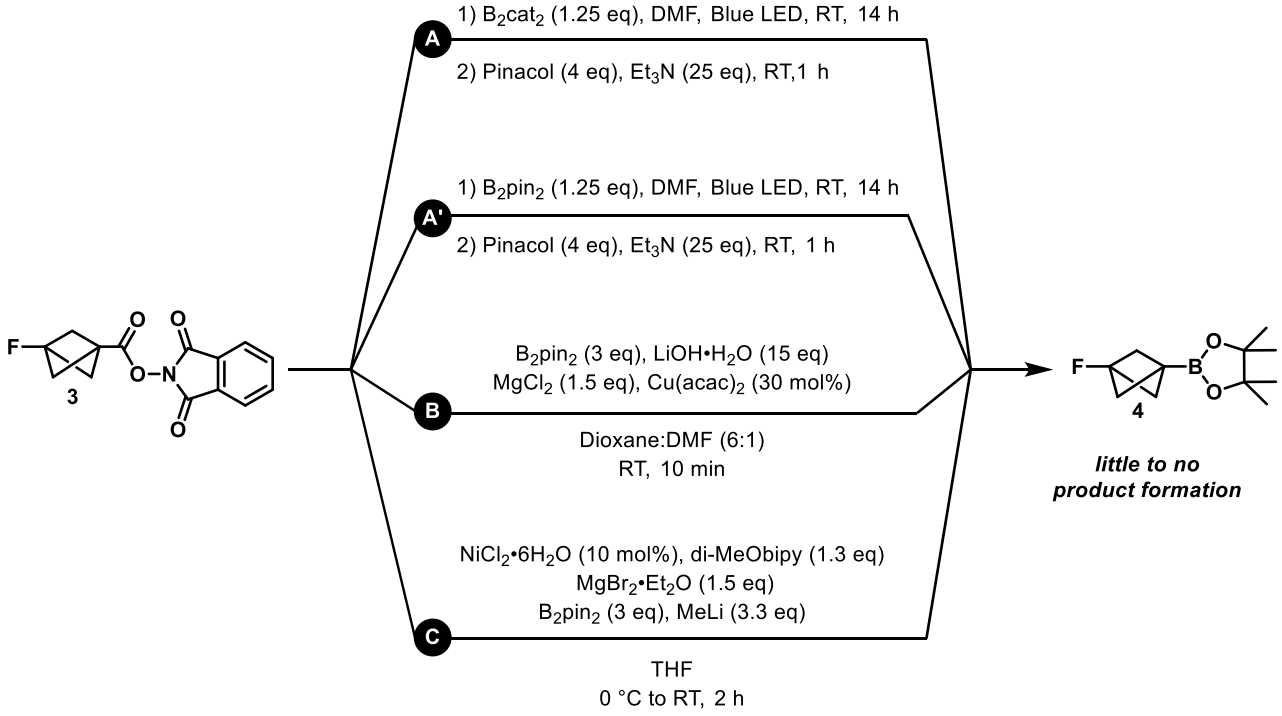


*Scheme 4: Summary of the different methods tried in attempts to form F-BCP-Bpin **4**.*

With many different attempts to form F-BCP-Bpin (**4**) being unsuccessful, it was decided to try form a C–B bond on the BCP an alternate way.

We then attempted to follow a protocol to form a potassium trifluoroborate salt using a RAE as starting material.[25] The paper was ambiguous on many steps, so a model NHPI ester (**5**) was prepared and the model NHPI ester was used in a decarboxylative borylation reaction (**Scheme 5**) to form a trifluoroborate salt (**7**). The reaction was optimized using differing equivalents of $KHF_2$

and ratios of methanol to water. The optimized conditions used 2.5 eq $KHF_2$ and a 4:1 ratio of MeOH to $H_2O$ (0.1M) and yielded 79% of the desired product (**6**).

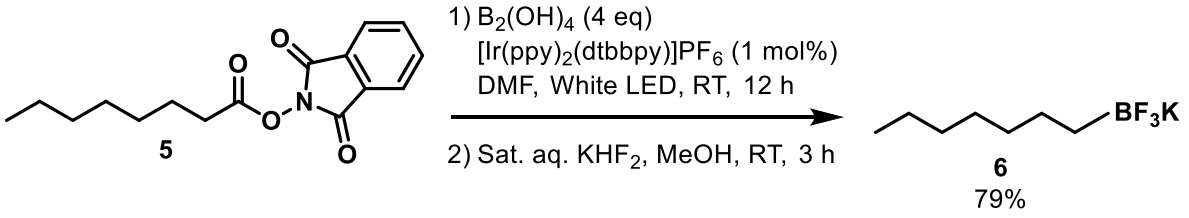


*Scheme 5: Decarboxylative borylation of model NHPI ester **6.***

The carefully determined parameters were then used in attempts to form **7** via decarboxylative fluorination (**Scheme 6**), results of which were unsuccessful.

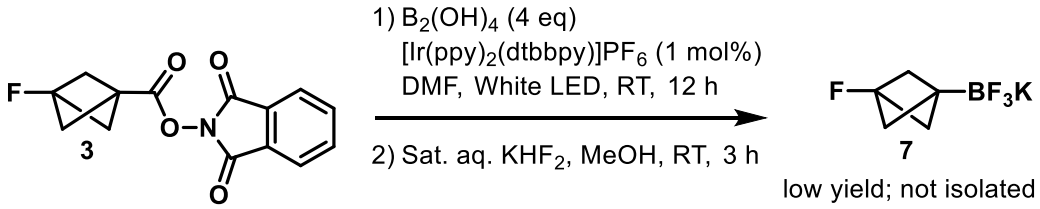


*Scheme 6: Decarboxylative borylation of F-BCP-NHPI ester **3.***

With the many attempts to form a C–B bond on our F-BCP species being unsuccessful, we decided to see if it would be possible to completely skip the need for a boron species to be used in cross-coupling reactions and rather proceed to a C–C bond formation direction starting from F-BCP-acid or F-BCP-NHPI. First attempts were done using conditions from a paper on nickel-catalyzed cross-coupling reactions of carboxylic acids.[26]

## 2.3 Nickel-catalyzed cross-coupling reactions with carboxylic acids

Many different attempts were done in attempts to form **8** via nickel-catalyzed cross-coupling reactions with alkyl halides. In total, five different alkyl halides were tried (**Scheme 7**); additionally, the base $K_2CO_3$ was exchanged for $Ag_2CO_3$ and $Na_2CO_3$.

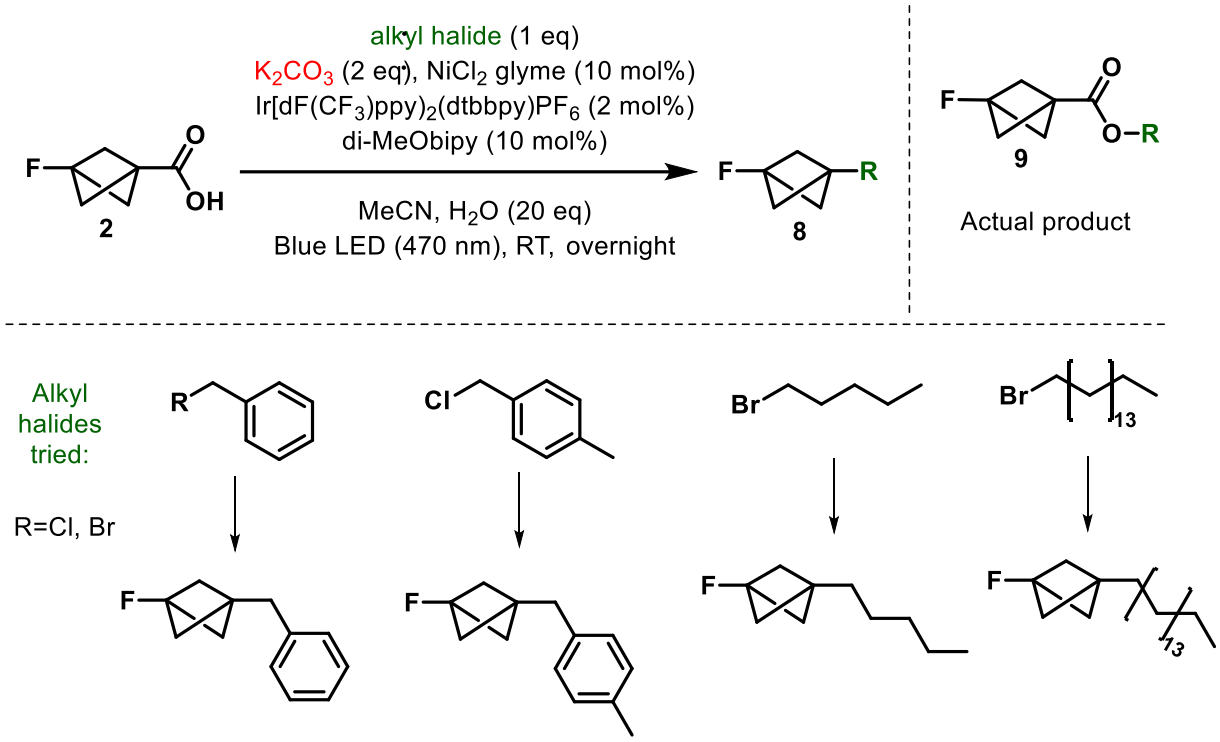


*Scheme 7: Nickel-catalyzed cross-coupling of F-BCP-Acid with alkyl halides.*

Unfortunately, all attempts resulted in the formation of the corresponding ester (**9**) and not the desired product (**8**), which was confirmed by isolation of the ester (**9**) by flash chromatography and further analysis by NMR spectrometry.

With the attempts to use F-BCP-Acid to form C–C bonds being unsuccessful, we then decided to attempt use the F-BCP-NHPI RAE to form C–C bonds as RAE are known to be able to form radical intermediates able to engage in coupling reaction.[19] The chosen method for the formation of C–C bonds using F-BCP-NHPI as our starting material was nickel-catalyzed decarboxylative Giese reactions, which will be discussed below.

## 2.4 Decarboxylative Giese reactions with F-BCP-NHPI

The formation of a C–C between the F-BCP and other compounds was attempted using decarboxylative Giese reactions, which use nickel-catalyzed fragmentation of NHPI RAEs to form C($sp^3$) radicals and then further reaction of those radicals with Michael acceptors.[27] Three different Michael acceptors were used; benzyl acrylate, butyl acrylate, and methyl acrylate (**Scheme 8**). Methyl acrylate was the most successful with a yield of 11%, followed by benzyl acrylate with 7%

yield, and butyl acrylate having the lowest yield of 2%. All yields were determined after purification of the compounds using silica gel chromatography.

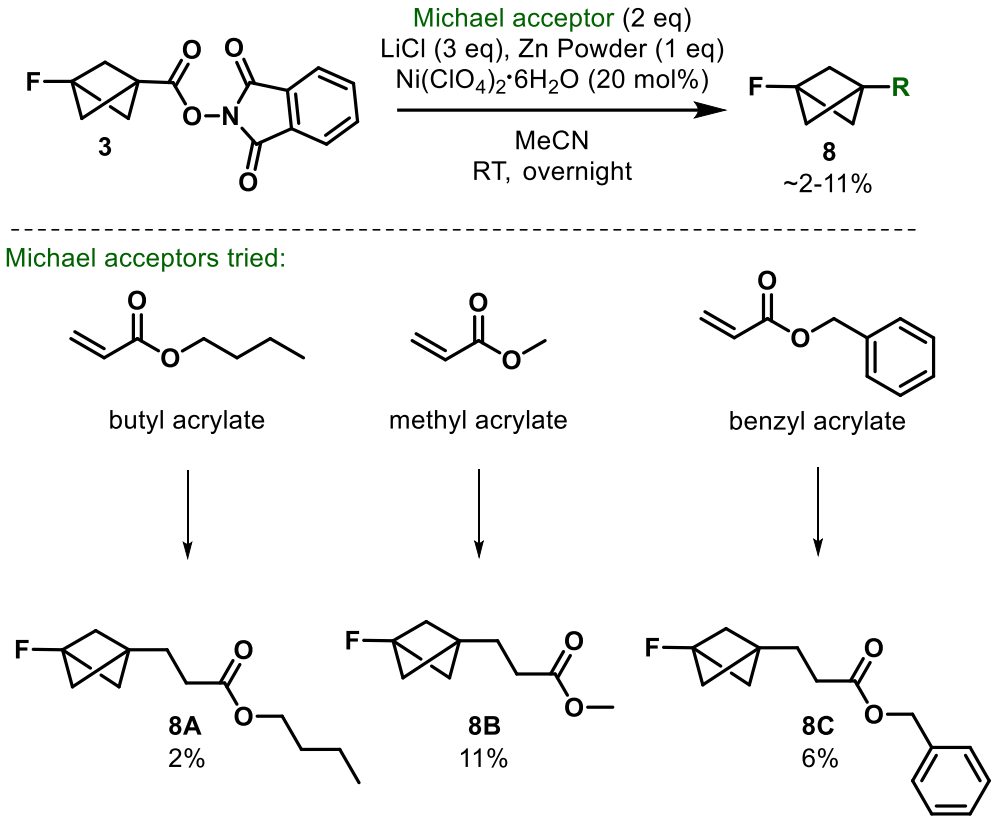


*Scheme 8: Nickel-catalyzed decarboxylative Giese reaction with F-BCP-NHPI.*

Given the success with the formation of compound **8A-C**, and the confirmation that C–C bonds can be made with BCPs, the desire to continue the investigation of this reaction was the basis of forming my honours thesis which will go into further explanation in the next section.

# 3. Research & Discussion

## 3.1 Mechanism for nickel-catalyzed decarboxylative Giese reactions

The proposed mechanism for the nickel-catalyzed decarboxylative Giese reactions first involves SET followed by fragmentation to form carbon dioxide, a R-BCP radical and a cyclic imide anion. The radical then reacts with the α,β-unsaturated carbonyl (Michael acceptor) for form a C–C bond (**Scheme 9**).

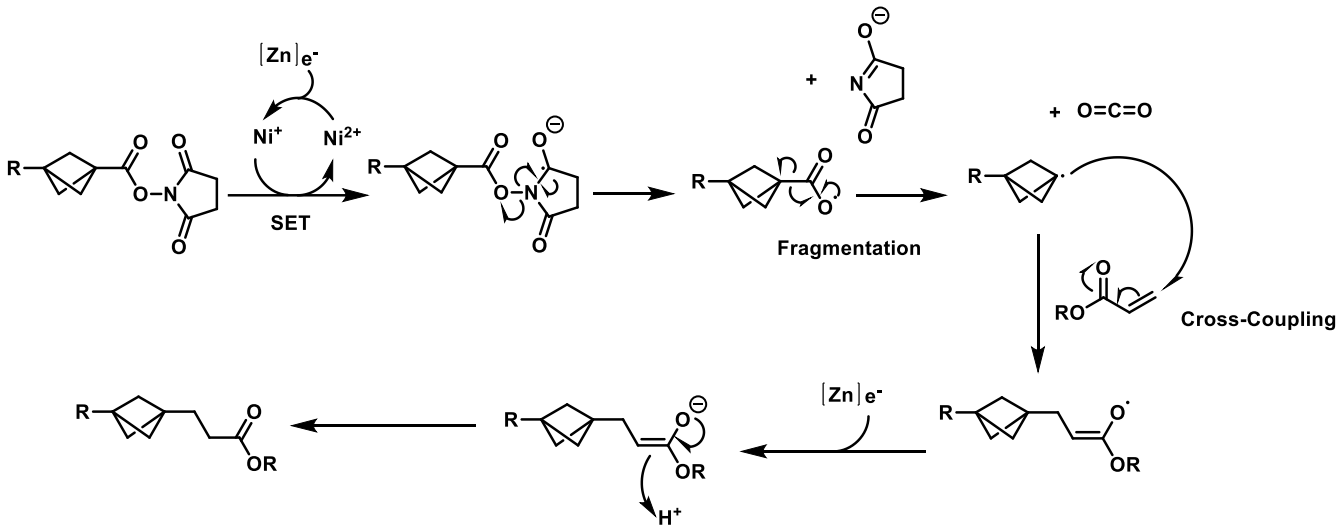


*Scheme 9: General pathway for nickel-catalyzed decarboxylative Giese reactions involving Michael acceptors and RAE.*

## 3.2 Preparation of Ester-BCP-Acid starting materials

In order to test if previous issues in the successful formation of products was due to the presence of fluorine, it was decided to replace the fluorine group for a methyl ester and test the methyl ester products in parallel with the fluorinated products. To do so, an ester-BCP-acid (**12**) had to be synthesized. Due to lack of commercial availability, and the cost of Ester-BCP-Acid, bicyclo[1.1.1]pentane-1,3-dicarboxylic acid (**1**) was used in an esterification reaction using thionyl chloride and methanol (**Scheme 10**) to form a diester BCP product (**10**) with a consistent yield around 98%.

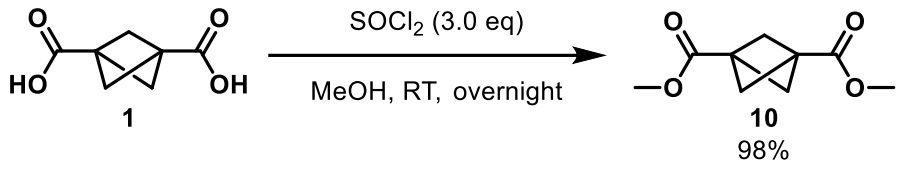


*Scheme 10: Esterification of dicarboxylic acid **1**.*

The diester BCP product (**10**) was than used to perform mono-saponification using $LiOH \cdot H_2O$ (**Scheme 11**) to afford the desired Ester-BCP-Acid product (**11**) with a yield of 70%. Saponification of a single ester is due to the product precipitating out as an carboxylate salt that is unable to react with the $LiOH \cdot H_2O$ a second time. The carboxylate salt is then converted to a free alcohol after the solution is acidified.

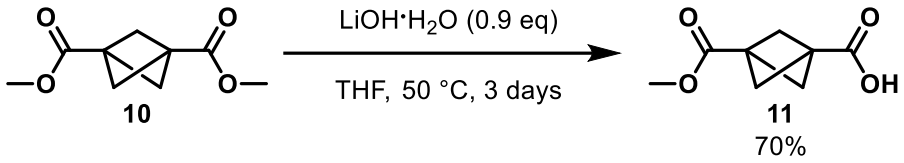


*Scheme 11: Selective saponification of diester with **10**.*

The synthesis of Ester-BCP-Acid (**12**) was done over two steps due to the ease of the reactions, high yields, and to prevent the formation of unusable product that would likely occur if the formation of the Ester-BCP-Acid (**12**) was attempted to be formed straight from the diacid (**1**). Attempts to form **2** over one step would likely form a combination of esterification products, which would likely require a complicated purification process to isolate the desired product (**11**), whereas over two steps the purification is easily done using liquid-liquid extraction.

### 3.3 Preparation of six RAE starting materials.

To test the effect of the type of RAE and the effect of the exchange of a fluorine group for a methyl ester, six different starting materials were made. All six starting materials, three containing a methyl ester and three different RAE groups (**14**, **15** and **16**), and three with fluorine and the same three RAE used for the methyl ester (**3**, **12**, and **13**), were synthesized using a Steglich

esterification reaction in which the BCP-Acid is reacted with a cyclic imide, a coupling agent (DIC), and a nucleophilic catalyst (DMAP) to form the desired RAE (**Scheme 12**).

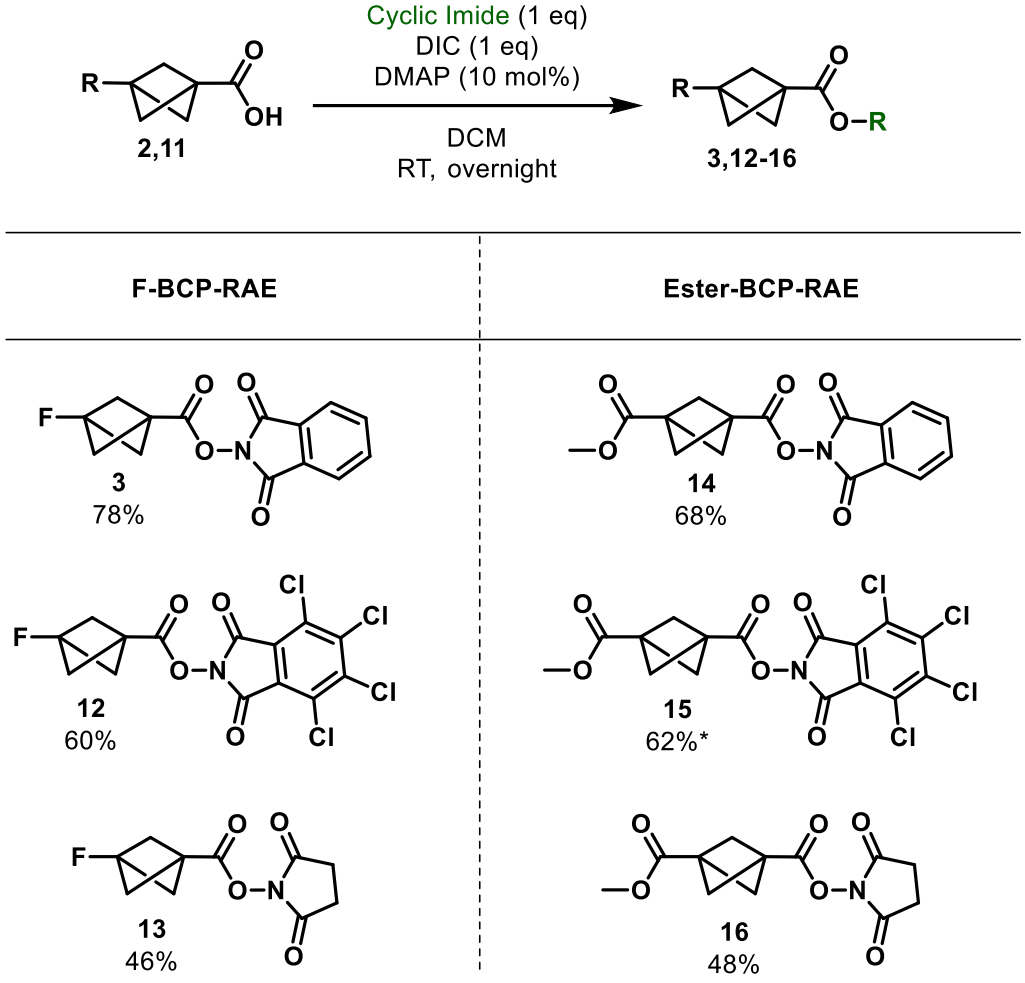


*yield should be higher as some impure fractions remained after column chromatography.

*Scheme 12: Steglich esterification reaction of R-BCP-acids with cyclic imides, DIC, and DMAP*

Compounds **3** and **12** were able to be purified with a single column using a mixture of DCM and hexane. Compounds **13** and **16** still contained starting material R-BCP-Acid (**2** and **11**) after the first column, so the compounds were washed with a 1:1 mixture of $H_2O$ and sat. $Na_2CO_3$ to remove the R-BCP-Acid starting material and afford the pure products. Compound **15** yielded a high yield of product (62%) after the first column, with impure fractions also collected that need to be purified via a second column. Compound **14** was successfully fully purified using two separate columns.

## 3.4 Nickel-catalyzed decarboxylative Giese reactions with the six starting material RAE

The first reaction done using the nickel-catalyzed decarboxylative Giese reaction was done with F-BCP-TCNHPI (**12**) and methyl acrylate (**Scheme 13**).

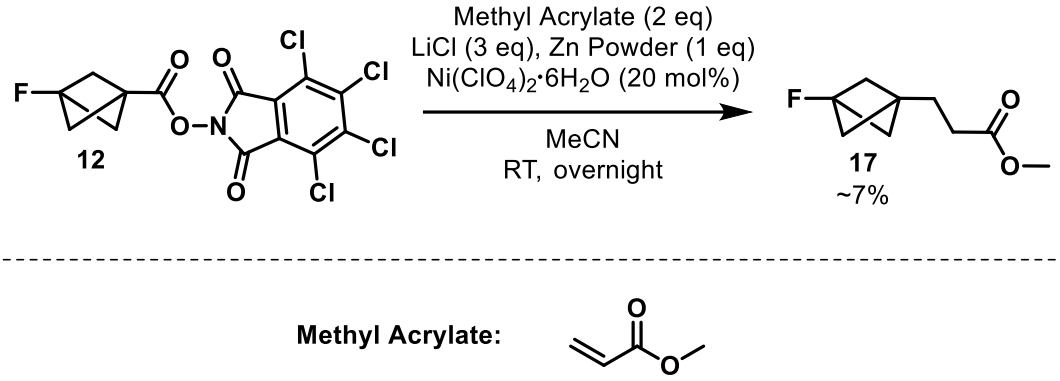


*Scheme 13: Nickel-catalyzed decarboxylative Giese reaction of F-BCP-TCNHPI with methyl acrylate.*

Analysis of the crude product using $^{1}H$ and $^{19}F$ NMR spectroscopy displayed that a new product had been formed with a shift in the starting material peak from -148.5 ppm to -145.7 ppm by $^{19}F$ NMR spectroscopy, and the shift of the doublet accounting for the BCP shifting from 2.62 ppm to 1.91 ppm in $^{1}H$ NMR spectroscopy. The product was then attempted to be isolated using a silica gel column of 5% EtOAc in Hexane, which yielded around 5 mg of product that was determined using $^{1}H$ NMR to still contain solvent and grease; the product was then placed on the vacuum line overnight in attempt to remove the solvent, and then reanalyzed by $^{1}H$ NMR spectroscopy to determine that the product was volatile, as the product was no longer present in the flask. It was then decided to order more Michael acceptors to use in the same reaction sequence, to see by using Michael acceptors that are heavier whether it would it be possible to form a product that is not volatile.

The first new Michael acceptor attempted was diethyl maleate, and it was reacted with F-BCP NHPI in a nickel-catalyzed decarboxylative Giese reaction (**Scheme 14**).

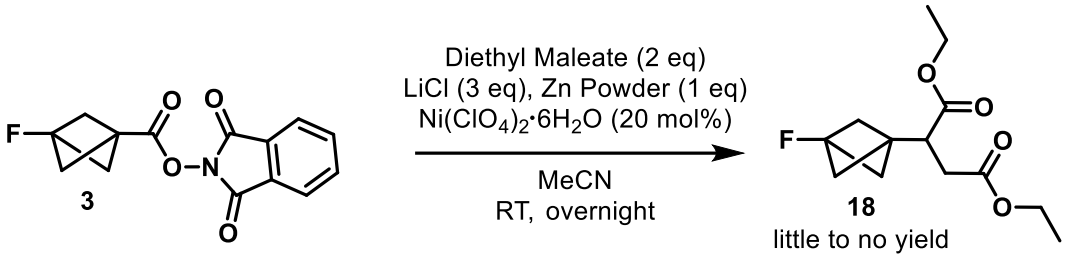


*Scheme 14: Nickel-catalyzed decarboxylative Giese reaction of F-BCP-NHPI with diethyl maleate.*

Two reactions were done to test if the order at which the Michael acceptor (diethyl maleate) is added has any effect on the reaction, with it either being added before the solvent, or after. Both reactions were unsuccessful, with the $^{1}$H NMR spectrum primarily showing unreacted diethyl maleate as well as the reduction product of diethyl maleate, diethyl succinate (**Figure 8**).

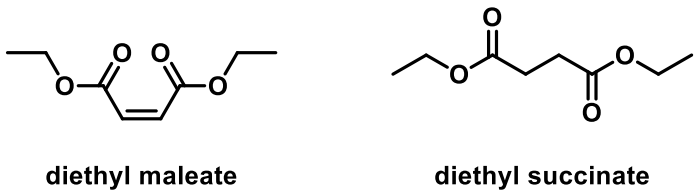


*Figure 8: Structure of diethyl maleate and its reduction product diethyl succinate.*

The reduction of the Michael acceptor was not noticed until the end of my honours thesis, or else parameters would have been altered in attempt to mitigate the proton donors in the reaction such as the $Ni(ClO_4)_2 \cdot 6H_2O$ or the solvent MeCN. Indeed, either of them may not be sufficiently dry, therefore introducing moisture that is causing undesired side reactions. The presence of residual oxygen may also be an issue. It could also be beneficial to test out different electron donors other than zinc.

Three different Michael acceptors (dimethyl fumarate, phenyl methacrylate, and methyl (*E)*-cinnamate) were then analyzed using the F-BCP-NHPI and Ester-BCP-NHPI in the same reaction conditions as was used for the dimethyl maleate (**Scheme 15**).

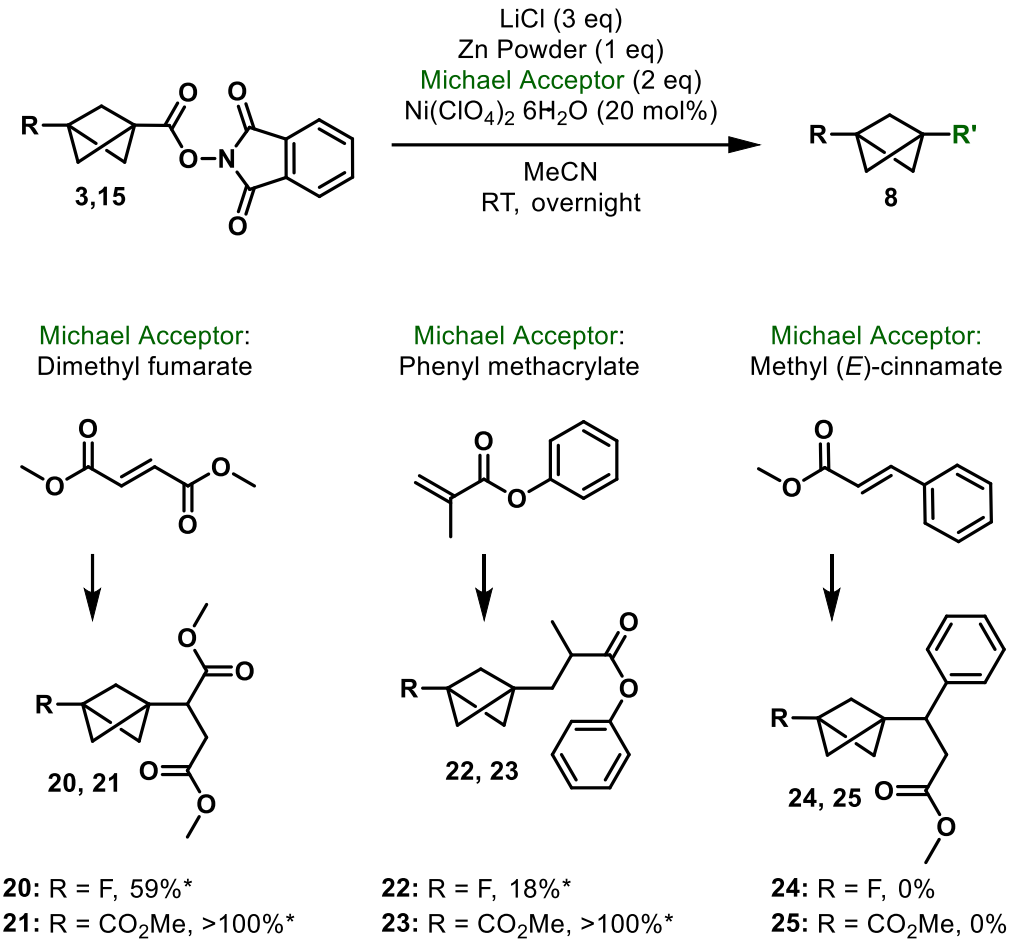


*Yields were determined using an internal standard (diglyme) which was later determined to be unsuitable.

*Scheme 15: Nickel-catalyzed decarboxylative Giese reaction of F-BCP-NHPI and Ester-BCP NHPI with dimethyl fumarate, phenyl methacrylate, and methyl (E)-cinnamate.*

All the products were analyzed by $^{1}$H NMR spectroscopy using an internal standard, but the chosen internal standard (diglyme) was determined to be an unsuitable internal standard as using it to calculate yield resulted in >100% yields, which would indicate that the internal standard (diglyme) had likely partially evaporated. Diglyme has a boiling point around 161°C,[28] which we believed would be high enough that the internal standard would not evaporate when added to the crude compound mixture and concentrated on the rotary evaporator. Disregarding the internal standard, the NMR spectra for **20-23** showed the successful formation of their respective products. Reactions with dimethyl fumarate appeared to have formed more product, which was determined by comparing the heights of the peaks present for unreacted Michael acceptor to the peak present for

the BCP on the $^1$H NMR spectrum. Due to that, dimethyl fumarate was chosen as the Michael acceptor to proceed forward with.

To determine an accurate yield of the dimethyl fumarate products **20** and **21**, both products were attempted to be isolated using silica gel chromatography. The fluorinated product (**20**) was isolated with small peaks of solvent and grease seen on the $^1$H NMR spectrum but was also determined to be volatile as the product was once again lost when placed under vacuum overnight. Product **21** was attempted to be isolated by three different columns, which included many different TLCs trying to determine appropriate solvent conditions and stains such as *p*-anisaldehyde, potassium permanganate, bromocresol green, phosphomolybdic acid (PMA), iodine, cerium ammonium molybdate (CAM), and vanillin, all of which led to the conclusion that the product is not stain active, and any attempt to isolate it will be very difficult. This difficulty could be overcome by synthesizing a starting material that contains a UV-active substituent, that after reaction with the Michael acceptors would still be present, allowing for the product to be visually seen on a TLC using UV light.

Due to the low yield and volatility of **20,** and the inability to isolate **21**, it was decided to use different internal standards to try to determine a more accurate yield. The chosen internal standards were 2-fluoro-4-nitrotoluene for the F-BCP products, and 1,3-dimethoxybenzene for the ester-BCP products (**Figure 9**).

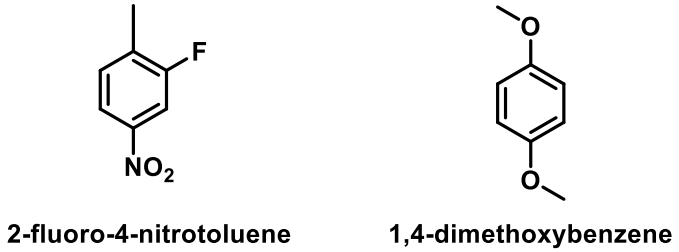


*Figure 9: Structures of internal standards 2-fluoro-4-nitrotoluene and 1,4-dimethoxybenzene.*

Using these internal standards in place of diglyme, we were able to determine yields of all six RAE reaction with dimethyl fumarate in a nickel-catalyzed decarboxylative Giese reaction (**Scheme 16**) to form **20** and **21**.

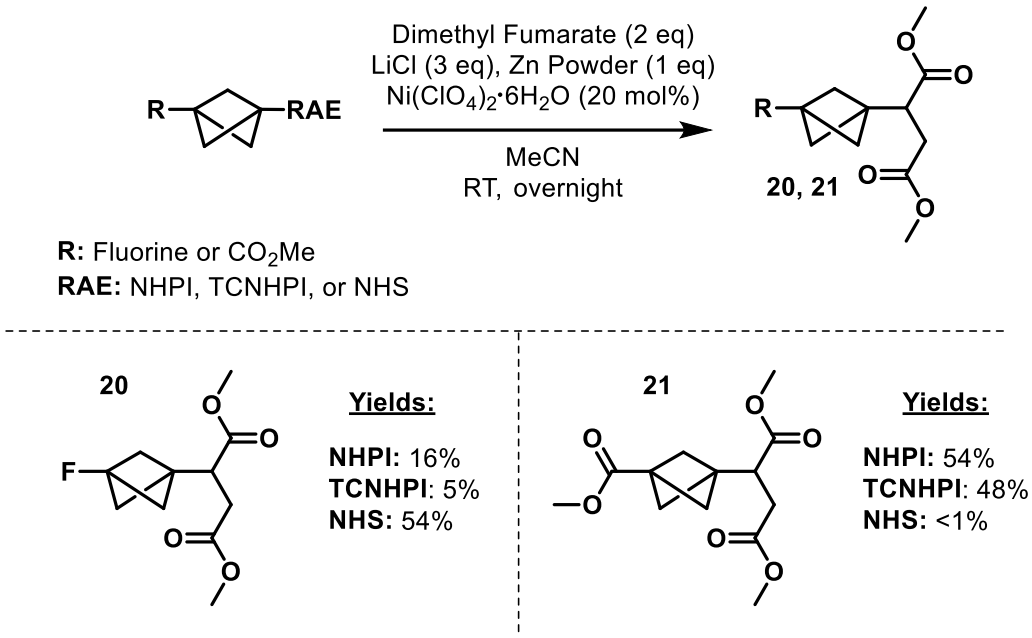


*Scheme 16: Nickel-catalyzed decarboxylative Giese reaction of R-BCP-RAEs and dimethyl fumarate.*

It was expected that use of NHPI as the cyclic imide would result in the highest yield, as that is what the literature this work is based on observed.[27] That is what is seen for the ester product (**21**), but for the fluorinated product (**20**) the best yield is seen when using NHS as the cyclic imide. This is likely due to the rate at which the radical is being formed, as well as the rate at which the radical is reacting with the Michael acceptor.

We were then interested in whether the presence of any air played a part in the partial success of the reactions, and if the yields could be improved by setting up the reactions in a glovebox under an inert environment. To do so, all the compounds needed for the reaction were weighed into 4-mL vials and then taken into the glovebox where the solvent would be added and the reaction stirred overnight. Two of the starting material RAE were chosen to be tested in the glovebox, the F-BCP-NHS RAE and the Ester-BCP-NHPI as they both had the highest yield of 54% (**Scheme 16**). Reactions of both RAE with dimethyl fumarate in nickel-catalyzed decarboxylative Giese reactions were then set up in the glovebox and ran in parallel (**Scheme 17**).

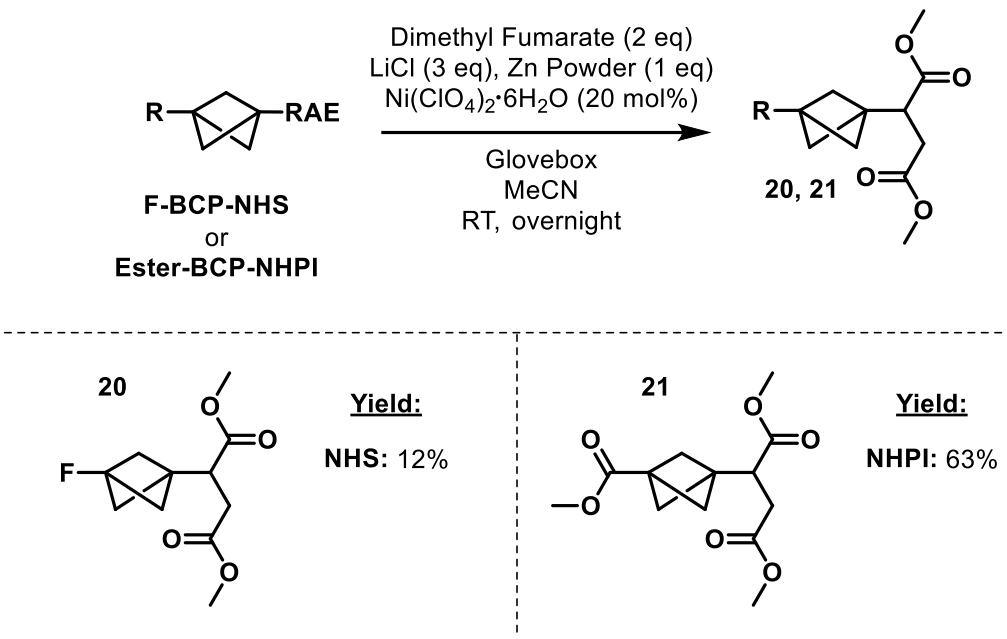


*Scheme 17: Nickel-catalyzed decarboxylative Giese reaction of F-BCP-NHS and Ester-BCP-NHPI with dimethyl fumarate, done in the glovebox.*

There was a decrease in yield from 54% to 12% between the reaction done with F-BCP-NHS outside of the glovebox and the reaction done in the glovebox, while the reaction done with the Ester-BCP-NHPI as the starting material had an increase in yield from 54% to 63% (**Scheme 16, 17**). All the nickel-catalyzed decarboxylative Giese reactions are done on the 0.2 mmol scale, making the difference between 54% and 63% very small and only about 5 mg product difference between the two, whereas the difference between 54% and 12% for the fluorinated product (**20**) accounts to about a 20 mg of product, which is more substantial and indicative that the glovebox influenced the reaction.

It would be beneficial to rerun both reactions with the same starting materials (**Scheme 17**) both in and outside of the glovebox to confirm whether the values collected for the product yields are reproducible and representative of the success rate of the reactions.

## 3.5 Nickel-catalyzed cross-coupling reactions of F-BCP-Acid with alkyl halides

During the first semester of my honours thesis, it was discovered by a graduate student (Stacie Nelson) that the reactions previously done using with blue light (470 nm) for photocatalyzed decarboxylative borylation reactions (**Scheme 4**) were supposed to be ran using an indigo light

(450 nm), which has a shorter wavelength and higher energy than blue light.[21] She then went on to retry the decarboxylative borylation reactions using an indigo light with a wavelength of 445 nm, and had success in forming Ester-BCP-Bpin products. With her success, I was curious if other reactions that we had previously done using blue light would work if done using indigo light. To test that hypothesis, F-BCP-Acid was reacted in a nickel-catalyzed decarboxylative reaction with benzyl chloride under indigo light (**Scheme 18**).

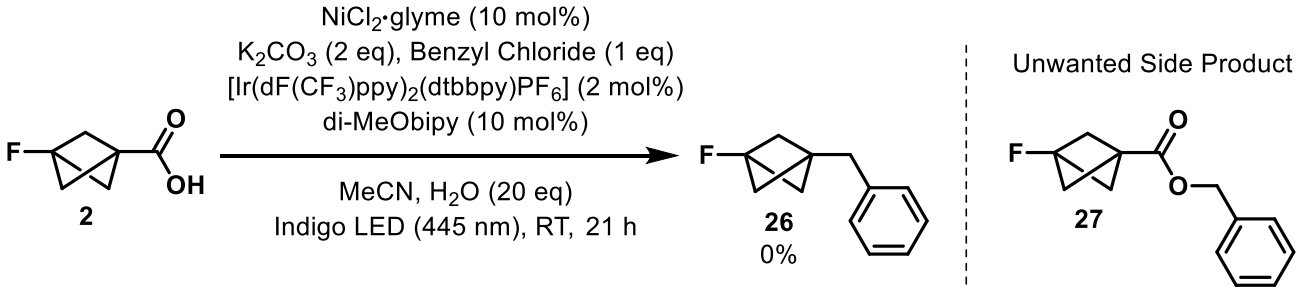


*Scheme 18: Nickel-catalyzed cross-coupling of F-BCP-Acid (**2**) with benzyl chloride.*

The reaction was still unsuccessful when using an indigo light in place of the blue light, with the formation of the unwanted ester product (**27**). Confirmation of the formation of **27** was done through purification of the compound by column chromatography, and then analysis by $^{1}$H NMR spectroscopy, where the location of the benzylic hydrogens was at 5.18 ppm, which is indicative of their proximity to a deshielding group like what is found in compound **27** and not in **26**. The benzylic hydrogens in **26** would be expected to be further upfield closer to 2 ppm.

## 3.6 X-ray crystallography of F-BCP-RAE

With the help of Miriam van Hoeve, the F-BCP-TCNHPI and F-BCP-NHS crystals were analyzed using x-ray crystallography. The F-BCP-NHPI product was previously analyzed by Jean-Denys Hamel in 2021. The results of all three crystals were interpreted and used to determine the relative strength of O–N bonds and C–F bonds present in each of the three compounds (**Figure 10**).

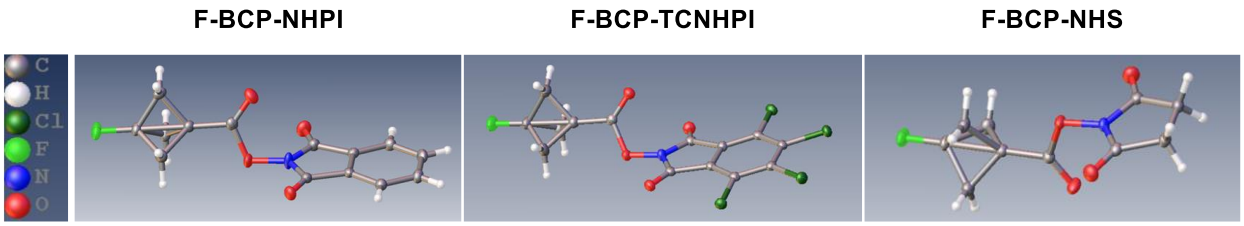


| | F-BCP-NHPI | F-BCP-TCNHPI | F-BCP-NHS |
|---|---|---|---|
| **O–N bond length:** | 1.3873 Å | 1.3800 Å | 1.3865 Å |
| **C–F bond length:** | 1.3721 Å | 1.3710 Å | 1.3725 Å |

*Figure 10: Crystal structure of F-BCP-NHPI, F-BCP-TCHNPI, F-BCP-NHS, and their corresponding bond lengths for C–F bonds and O–N bonds. Thermal ellipsoids were set to a default 50%. The corresponding colours for the crystal structures are grey = carbon, white = hydrogen, dark green = chlorine, light green = fluorine, blue = nitrogen, and red = oxygen.*

The F-BCP-NHPI has the longest O–N bond at 1.3873 Å and F-BCP-NHS being very similar in length at 1.3865 Å. F-BCP-TCNHPI has the shortest O–N bond, which could indicate that the fragmentation that occurs for reductive decarboxylative reactions of NHPI esters (**Scheme 1**) may be easier and quicker for the NHPI and NHS RAE than the TCNHPI RAE, as the strength of the bond is typically inverse to its length.

# 4. Conclusion

## 4.1 Nickel-catalyzed decarboxylative Giese reactions

This honours thesis has been able to prove that F-BCPs and Ester-BCPs can be converted into radicals that will react with α,β-unsaturated carbonyls (Michael acceptors) to form C–C bonds using nickel-catalyzed decarboxylative Giese reactions. The issue still remains in forming a product that is stable enough to be purified using column chromatography, as well as a product that would be stain active.

## 4.2 Nickel-catalyzed cross-coupling of carboxylic acids with alkyl halides

The use of F-BCP-Acid as a starting material for nickel-catalyzed cross-coupling reactions with alkyl halides has proved to be difficult and unsuccessful, with every reaction forming the undesired ester product (**10**).

# 5. Future work

The nickel-catalyzed decarboxylative Giese reactions could be optimized to determine if there is a way to decrease C=C bond reduction (saturation) of the Michael acceptor as a side reaction. This could be done by changing the previously used nickel catalyst, $Ni(ClO_4)_2 \cdot 6H_2O$, to a non-hydrated nickel catalyst. One potential that is already available in the Hamel research lab is $NiCl_2 \cdot$glyme. Optimization could also be done by testing the effect of the solvent used, as well as trying different electron donors in place of zinc powder.

Another interesting avenue to pursue would be if a UV active substituent such as a benzene ring could be added onto the ester-BCP product, so that upon reacting with the Michael acceptor the product would likely be UV-active and easier to attempt to purify using column chromatography. This could potentially be done by swapping the methanol for phenol in the reaction involving the esterification of dicarboxylic acid using $SOCl_2$ (**Scheme 19**), but further research would need to be done to confirm that hypothesis.

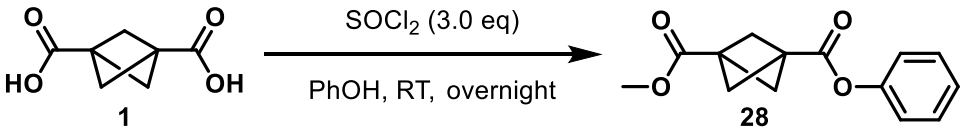


*Scheme 19: Proposed synthesis of a BCP substituted with a methyl ester and phenol ester **28**..*

# 6. Experimental and characterization

## 6.1 General Comments

All reactions were carried out under a nitrogen atmosphere. THF, DCM, toluene, MeCN, and benzene were purified using an MBraun solvent purification system (SPS). All other commercially available compounds were used as received. Vials (Fischer Scientific) used to perform reactions were capped with Qorpak thermoset PTFE caps. Photo-irradiation was carried out with a Lumidox II LumLamp (3.5 W, 470 nm). Thin layer chromatography (TLC) analysis of reaction mixtures was performed using Silicycle silica gel 60 Å F254 TLC plates, and the plates were visualized under UV light or by staining with phosphomolybdic acid (PMA), cerium ammonium molybdate (CAM), or *p*-anisaldehyde. Flash column chromatography was carried out on Silicycle silica gel 60 Å, 230-400 mesh. $^{1}H$, $^{13}C$ and $^{19}F$ NMR spectra were recorded in $CDCl_3$ at room temperature using a Bruker Avance II (300 MHz for $^{1}H$, 282 MHz for $^{19}F$) or Avance III (700 MHz for $^{1}H$, 176 MHz for $^{13}C$, 659 MHz for $^{19}F$) NMR spectrometer. $^{1}H$ and $^{13}C$ NMR chemical shifts are reported downfield of tetramethylsilane and are respectfully referenced to tetramethylsilane (δ = 0.00 ppm) and chloroform (δ = 77.16 ppm). Multiplicities are reported using the following abbreviations: s = singlet, d = doublet, t = triplet, q = quartet, sept. = septet, m = multiplet, bs = broad singlet.

## 6.2 Synthesis of Ester-BCP-Acid

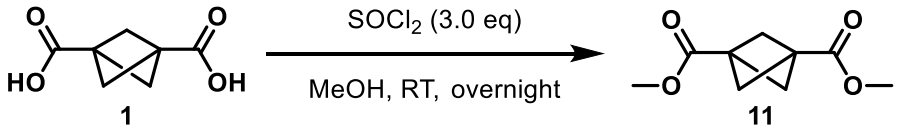


**dimethyl bicyclo[1.1.1]pentane-1,3-dicarboxylate (11):** Bicyclo[1.1.1]pentane-1,3-dicarboxylic acid (2000 mg, 12.81 mmol) was dissolved in MeOH (32 mL). Then $SOCl_2$ (2.8ml, 38.43 mmol) was added dropwise, and the solution stirred at RT overnight. A 1:1 solution of hexane and $Et_2O$ (10 mL) was added and then the mixture filtered through a frit containing silica (2.5 g). The filtrate was transferred to a Sept funnel using DCM, and then an equivalent volume of $NaHCO_3$ added. The mixture was then extracted with EtOAc (3x), dried with MgSO4, filtered, and concentrated *in vacuo*. The desired product (2314 mg, 98%) was isolated as a white solid. Spectroscopic data was in agreement with the literature.[29]

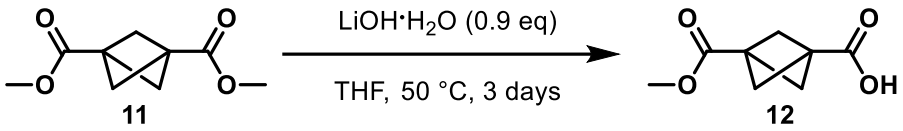


**3-(methoxycarbonyl)bicyclo[1.1.1]pentane-1-carboxylic acid (12):** compound 11 (1.0 eq), and $LiOH \cdot H_2O$ (0.9 eq) were dissolved in THF (0.5 M), and then stirred at 50°C for 3 days. Water was then added until the precipitate was fully dissolved, and then transferred to a sept funnel using water and DCM. The mixture was washed with DCM (3x), pH adjusted using conc. HCl (pH <3), extracted with DCM (3x), dried with $Na_2SO_4$, filtered, and concentrated *in vacuo*. The desired product (1531 mg, 70%) was isolated as a white solid. Spectroscopic data was in agreement with the literature.[29]

## 6.3 Synthesis of F-BCP-Acid

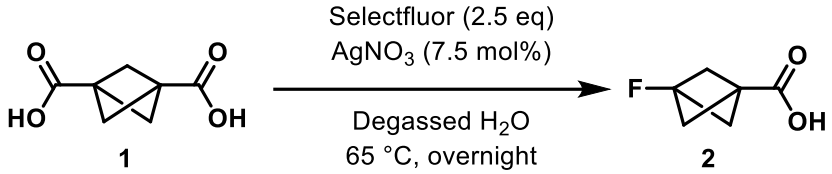


**3-fluorobicyclo[1.1.1]pentane-1-carboxylic acid (2):** Bicyclo[1.1.1]pentane-1,3-dicarboxylic acid (780.7 mg, 5 mmol), Selectfluor (4428.3 mg, 12.5 mmol), and $AgNO_3$ (63.7 mg, 0.375 mmol) were added to a RBF and a small condenser installed. The system was then purged for 10 minutes with $N_2$. Degassed $H_2O$ (35.4 mL) was added and then the mixture stirred at 65 °C overnight. The mixture was then filtered using a frit, and the filtrate was extracted with $Et_2O$ (3x), dried with $Na_2SO_4$, filtered, and concentrated *in vacuo*. The solid was isolated via trituration with pentane, filtered, and concentrated using *in vacuo*. The desired product (467 mg, 72%) was isolated as a white solid. Spectroscopic data was in agreement with the literature.[29]

## 6.4 Synthesis of RAE by Steglich esterification

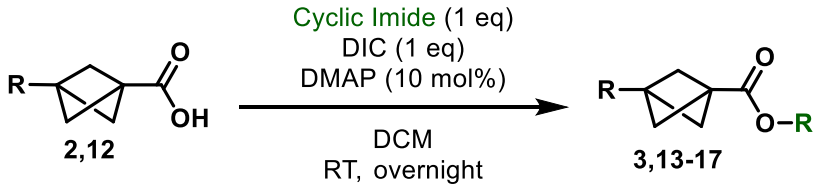


**Procedure for Synthesis of RAE by Steglich esterification using carboxylic acids and cyclic imides (General Procedure A):** Compound 2 or 12 (1 eq), DMAP (10 mol %), were dissolved in DCM (0.1 M) and then the system purged until nitrogen for 10 minutes. DIC (1.0 eq) was added and then the mixture stirred at RT overnight. The mixture was then concentrated *in vacuo*. Desired products were then isolated as white solids by flash chromatography.

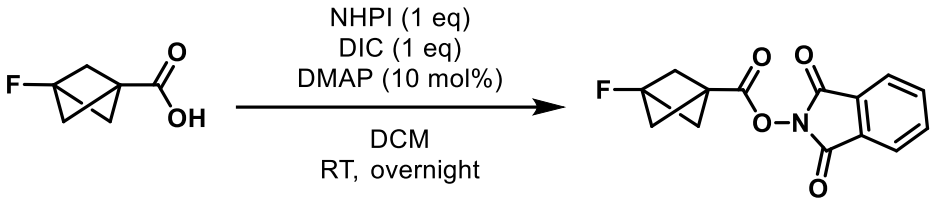


**1,3-dioxoisoindolin-2-yl 3-fluorobicyclo[1.1.1]pentane-1-carboxylate ( ):** The RAE F-BCP-NHPI was prepared following procedure A for the Steglich esterification of **2**. On a 4.756 mmol scale, the product (1021 mg, 78%) was isolated as a white solid by flash chromatography using 75% DCM/Hexane. $^{1}$H NMR (700 MHz, $CDCl_3$) δ 7.90 (m, 2H) δ 7.81 (m, 2H) δ 2.62 (d, 6H, J = 2.3 Hz); $^{13}$C NMR (176 Hz, $CDCl_3$) δ 161.62, 134.87, 128.83, 124.08, 55.55, 56.42, 26.35, 26.05; $^{19}$F NMR (282 MHz, $CDCl_3$) δ -148.5 (s, 1F); X-ray data recorded as JD21001.

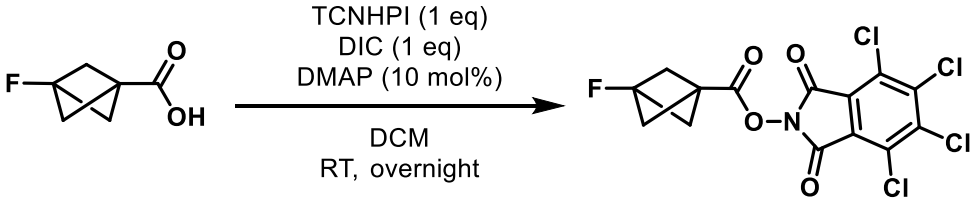


**4,5,6,7-tetrachloro-1,3-dioxoisoindolin-2-yl 3-fluorobicyclo[1.1.1]pentane-1-carboxylate ( ):** The RAE F-BCP- TCNHPI was prepared following procedure A for the Steglich esterification of

**2**. On a 1.537 mmol scale, the product (380 mg, 60%) was isolated as a white solid by flash chromatography using 58% DCM/Hexane. $^{1}$H NMR (700 MHz, $CDCl_3$) δ 2.62 (d, 6H, J = 2.2 Hz); $^{13}$C NMR (176 Hz, $CDCl_3$) δ 164.8 (d, $J_{C-F}$ = 38.8 Hz), 157.4, 141.3, 130.7, 124.7, 74.5 (d, $J_{C-F}$ = 329 Hz), 56.7 (d, $J_{C-F}$ = 22.5 Hz), 26.3 (d, $J_{C-F}$ = 51.8 Hz); $^{19}$F NMR (659 MHz, $CDCl_3$) δ -148.5 (sept, 1F, J = 2.3 Hz); X-ray data recorded as JDH24001.

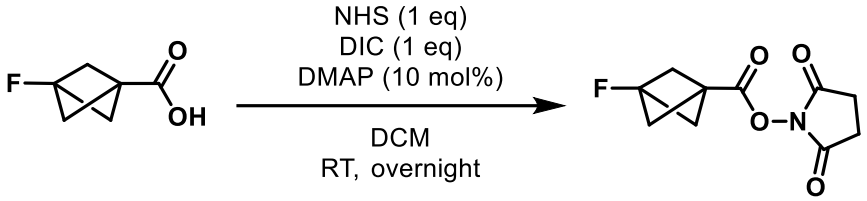


**2,5-dioxopyrrolidin-1-yl 3-fluorobicyclo[1.1.1]pentane-1-carboxylate ( ):** The RAE F-BCP-NHS was prepared following procedure A for the Steglich esterification of **2**. On a 1.537 mmol scale, the product (162 mg, 46%) was isolated as a white solid by flash chromatography using 30% EtOAc/Hexane following by a wash with a 1:1 mixture of $H_2O$ and sat. $Na_2CO_3$. $^{1}$H NMR (700 MHz, $CDCl_3$) δ 2.85 (bs, 4H), 2.57 (d, 6H, J = 2.3 Hz); $^{13}$C NMR (176 Hz, $CDCl_3$) δ 168.9, 164.2 (d, $J_{C-F}$ = 38.8 Hz), 74.6 (d, $J_{C-F}$ = 329 Hz), 56.6 (d, $J_{C-F}$ = 22.5 Hz), 26.3 (d, $J_{C-F}$ = 51.5 Hz), 25.7; $^{19}$F NMR (659 MHz, $CDCl_3$) δ -148.7 (sept, 1F, J = 2.3 Hz); X-ray data recorded as JDH24002.

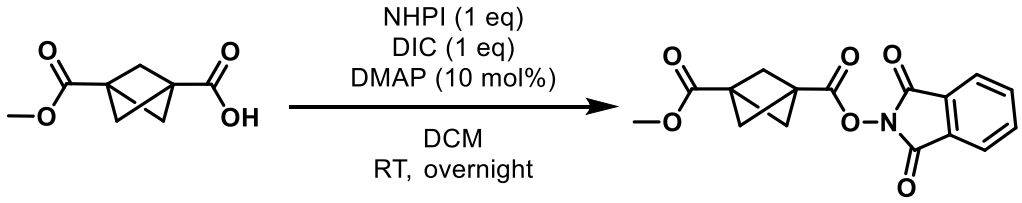


**1-(1,3-dioxoisoindolin-2-yl) 3-methyl bicyclo[1.1.1]pentane-1,3-dicarboxylate ( ):** The RAE Ester-BCP-NHPI was prepared following procedure A for the Steglich esterification of **12**. On a 2.43 mmol scale, the product (522 mg, 68%) was isolated as a white solid by flash chromatography using 30% EtOAc/Hexane. $^{1}$H NMR (700 MHz, $CDCl_3$) δ 7.89 (m, 2H), 7.80 (m, 2H), 3.72 (s, 3H), 2.56 (m, 6H); $^{13}$C NMR (176 Hz, $CDCl_3$) δ 169.0, 164.9, 161.8, 135.0, 129.0, 124.2, 53.7, 52.2, 38.7, 35.5.

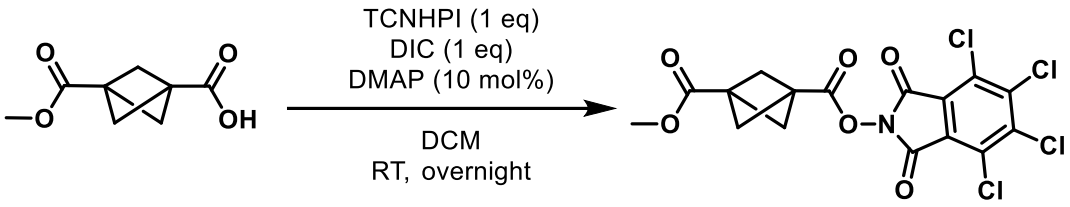


**1-methyl 3-(4,5,6,7-tetrachloro-1,3-dioxoisoindolin-2-yl) bicyclo[1.1.1]pentane-1,3-dicarboxylate ( ):** The RAE Ester-BCP-TCNHPI was prepared following procedure A for the Steglich esterification of **12**. On a 1.175 mmol scale, the product (331 mg, 62%) was isolated as a white solid by flash chromatography using 10% EtOAc/Hexane. $^{1}$H NMR (700 MHz, $CDCl_3$) δ 3.73 (s, 3H), 2.56 (s, 6H); $^{13}$C NMR (176 Hz, $CDCl_3$) δ 168.9, 164.4, 157.5, 141.3, 130.7, 124.8, 53.8, 52.2, 38.8, 35.4.

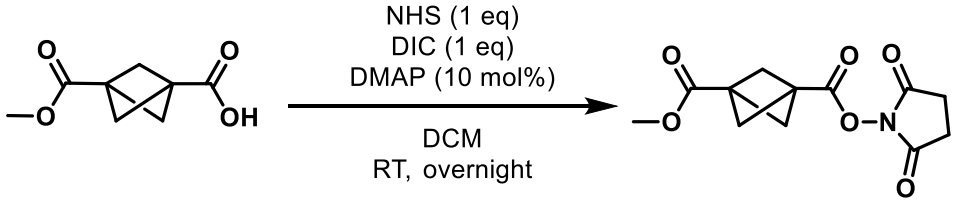


**1-(2,5-dioxopyrrolidin-1-yl) 3-methyl bicyclo[1.1.1]pentane-1,3-dicarboxylate ( ):** The RAE Ester-BCP-NHS was prepared following procedure A for the Steglich esterification of **12**. On a 1.175 mmol scale, the product (151mg, 48%) was isolated as a white solid by flash chromatography using 40% EtOAc/Hexane following by a wash with a 1:1 mixture of $H_2O$ and sat. $Na_2CO_3$. $^{1}$H NMR (700 MHz, $CDCl_3$) δ 3.71 (s, 3H), 2.85 (bs, 4H), 2.51 (s, 6H); $^{13}$C NMR (176 Hz, $CDCl_3$) δ 168.97. 168.95, 163.9, 53.7, 52.2, 38.7, 35.5, 25.7.

## 6.5 Nickel-catalyzed decarboxylated Giese reactions with RAE

**Procedure for Nickel-catalyzed decarboxylated Giese reactions of RAE with Michael acceptors (General Procedure B):** LiCl (3.0 eq), RAE (1.0 eq), Zn powder (2.0 eq), and $Ni(ClO_4)_2 \cdot 6H_2O$ (20 mol%) were added to a test tube, and then the test tube evacuated and backfilled with nitrogen (3x), followed by addition of Michael acceptor (2.0 eq) via syringe. Dry

MeCN (0.4 M) was then added, and the mixture stirred at RT overnight. The mixture was then added to 20 mL of 1:1 v/v solution of distilled $H_2O$ and aq. $NH_4Cl$ solution, extracted with $Et_2O$ (3x), dried with $MgSO_4$, filtered, and concentrated *in vacuo*. The desired products were then identified using NMR spectroscopy.

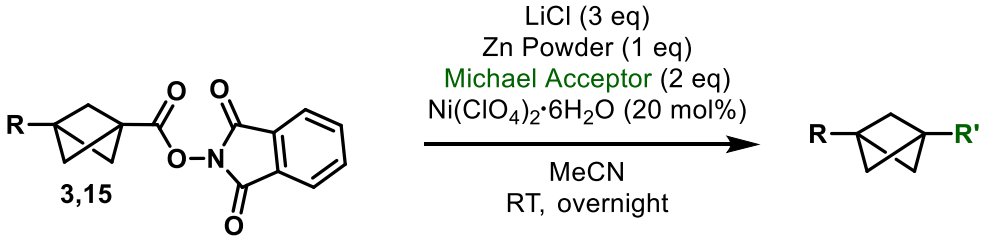


products successfully observed by $^1H$ and $^{19}F$ NMR spectroscopy; key NMR resonances provided ($^1H$ = BCP only)

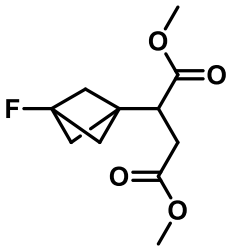


$^1H$ (300 MHz) δ 1.98 (d, 6H)
$^1H$ (700 MHz) δ 1.98 (s, 6H)
$^{19}F$ (282 MHz) δ -149.0 (s, 1F)

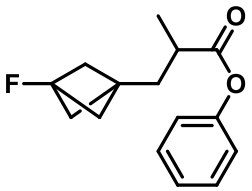


$^1H$ (300 MHz) δ 2.00 (m, 6H)
$^1H$ (700 MHz) δ 2.00 (dm, 6H)
$^{19}F$ (282 MHz) δ -145.2 (s, 1F)

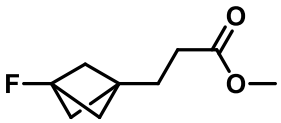


$^1H$ (300 MHz) δ 1.91 (d, 6H)
$^{19}F$ (282 MHz) δ -145.7 (s, 1F)

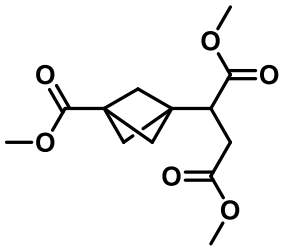


$^1H$ (700 MHz) δ 1.97 (s, 6H)

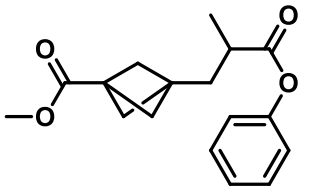


$^1H$ (300 MHz) δ 2.01 (s, 6H)
$^1H$ (700 MHz) δ 2.01 (m, 6H)

# 7. References


(1) Lowe, P. T.; O'Hagan, D. A role for fluorine in flavours, fragrances and pheromones. *Journal of Fluorine Chemistry* **2020**, *230*, 109420. DOI: https://doi.org/10.1016/j.jfluchem.2019.109420.
(2) Jeschke, P. The unique role of halogen substituents in the design of modern agrochemicals. *Pest Manage. Sci.* **2010**, *66* (1), 10-27. DOI: 10.1002/ps.1829.
(3) Chandra, G.; Singh, D. V.; Mahato, G. K.; Patel, S. Fluorine-a small magic bullet atom in the drug development: perspective to FDA approved and COVID-19 recommended drugs. *Chem Zvesti* **2023**, 1-22. DOI: 10.1007/s11696-023-02804-5 From NLM.
(4) Okazoe, T. Overview on the history of organofluorine chemistry from the viewpoint of material industry. *Proc Jpn Acad Ser B Phys Biol Sci* **2009**, *85* (8), 276-289. DOI: 10.2183/pjab.85.276 From NLM.
(5) O'Hagan, D. Understanding organofluorine chemistry. An introduction to the C-F bond. *Chem Soc Rev* **2008**, *37* (2), 308-319. DOI: 10.1039/b711844a From NLM.
(6) Shah, P.; Westwell, A. D. The role of fluorine in medicinal chemistry. *Journal of Enzyme Inhibition & Medicinal Chemistry* **2007**, *22* (5), 527-540, Article. DOI: 10.1080/14756360701425014 From EBSCOhost Academic Search Complete.
(7) Benedetto Tiz, D.; Bagnoli, L.; Rosati, O.; Marini, F.; Sancineto, L.; Santi, C. New Halogen-Containing Drugs Approved by FDA in 2021: An Overview on Their Syntheses and Pharmaceutical Use. *Molecules* **2022**, *27* (5). DOI: 10.3390/molecules27051643 From NLM.
(8) Dubowchik, G. M.; Conway, C. M.; Xin, A. W. Blocking the CGRP Pathway for Acute and Preventive Treatment of Migraine: The Evolution of Success. *J Med Chem* **2020**, *63* (13), 6600-6623. DOI: 10.1021/acs.jmedchem.9b01810 From NLM.
(9) Crapanzano, C.; Laurenzi, P. F.; Amendola, C.; Casolaro, I. Clinical perspective on antipsychotic receptor binding affinities. *Braz J Psychiatry* **2021**, *43* (6), 680-681. DOI: 10.1590/1516-4446-2021-2245 From NLM.
(10) Tarantino, G.; Hammond, C. Catalytic C(sp3)–F bond formation: recent achievements and pertaining challenges. *Green Chemistry* **2020**, *22* (16), 5195-5209. DOI: 10.1039/d0gc02067b.
(11) Subbaiah, M. A. M.; Meanwell, N. A. Bioisosteres of the Phenyl Ring: Recent Strategic Applications in Lead Optimization and Drug Design. *Journal of Medicinal Chemistry* **2021**, *64* (19), 14046-14128. DOI: 10.1021/acs.jmedchem.1c01215.
(12) Lovering, F.; Bikker, J.; Humblet, C. Escape from Flatland: Increasing Saturation as an Approach to Improving Clinical Success. *Journal of Medicinal Chemistry* **2009**, *52* (21), 6752-6756. DOI: 10.1021/jm901241e.
(13) Rein, M. J.; Renouf, M.; Cruz-Hernandez, C.; Actis-Goretta, L.; Thakkar, S. K.; da Silva Pinto, M. Bioavailability of bioactive food compounds: a challenging journey to bioefficacy. *Br J Clin Pharmacol* **2013**, *75* (3), 588-602. DOI: 10.1111/j.1365-2125.2012.04425.x From NLM.
(14) Burger, A. Isosterism and bioisosterism in drug design. *Prog Drug Res* **1991**, *37*, 287-371. DOI: 10.1007/978-3-0348-7139-6_7 From NLM.
(15) Wiberg, K. B.; Connor, D. S.; Lampman, G. M. The reaction of 3-bromocyclobutane-1-methyl bromide with sodium : bicyclo[1. 1. 1]pentane. *Tetrahedron Letters* **1964**, *5* (10), 531-534. DOI: https://doi.org/10.1016/S0040-4039(00)73269-2.
(16) Shire, B. R.; Anderson, E. A. Conquering the Synthesis and Functionalization of Bicyclo[1.1.1]pentanes. *JACS Au* **2023**, *3* (6), 1539-1553. DOI: 10.1021/jacsau.3c00014.
(17) Coric, V.; van Dyck, C. H.; Salloway, S.; Andreasen, N.; Brody, M.; Richter, R. W.; Soininen, H.; Thein, S.; Shiovitz, T.; Pilcher, G.; et al. Safety and tolerability of the γ-secretase inhibitor avagacestat in a phase 2 study of mild to moderate Alzheimer disease. *Arch Neurol* **2012**, *69* (11), 1430-1440. DOI: 10.1001/archneurol.2012.2194 From NLM.

(18) Bychek, R.; Mykhailiuk, P. K. A Practical and Scalable Approach to Fluoro-Substituted Bicyclo[1.1.1]pentanes. *Angewandte Chemie International Edition* **2022**, *61* (29), e202205103. DOI: https://doi.org/10.1002/anie.202205103.
(19) Azpilcueta-Nicolas, C. R.; Lumb, J. P. Mechanisms for radical reactions initiating from N-hydroxyphthalimide esters. *Beilstein J Org Chem* **2024**, *20*, 346-378. DOI: 10.3762/bjoc.20.35 From NLM.
(20) Murarka, S. N-(Acyloxy)phthalimides as Redox-Active Esters in Cross-Coupling Reactions. *Advanced Synthesis & Catalysis* **2018**, *360* (9), 1735-1753. DOI: https://doi.org/10.1002/adsc.201701615.
(21) Fawcett, A.; Pradeilles, J.; Wang, Y.; Mutsuga, T.; Myers, E. L.; Aggarwal, V. K. Photoinduced decarboxylative borylation of carboxylic acids. *Science* **2017**, *357* (6348), 283-286. DOI: 10.1126/science.aan3679 From NLM.
(22) Thomas, A. A.; Zahrt, A. F.; Delaney, C. P.; Denmark, S. E. Elucidating the Role of the Boronic Esters in the Suzuki-Miyaura Reaction: Structural, Kinetic, and Computational Investigations. *J Am Chem Soc* **2018**, *140* (12), 4401-4416. DOI: 10.1021/jacs.8b00400 From NLM.
(23) Wang, J.; Shang, M.; Lundberg, H.; Feu, K. S.; Hecker, S. J.; Qin, T.; Blackmond, D. G.; Baran, P. S. Cu-Catalyzed Decarboxylative Borylation. *ACS Catalysis* **2018**, *8* (10), 9537-9542. DOI: 10.1021/acscatal.8b02928.
(24) Li, C.; Wang, J.; Barton, L. M.; Yu, S.; Tian, M.; Peters, D. S.; Kumar, M.; Yu, A. W.; Johnson, K. A.; Chatterjee, A. K.; et al. Decarboxylative borylation. *Science* **2017**, *356* (6342). DOI: 10.1126/science.aam7355 From NLM.
(25) Hu, D.; Wang, L.; Li, P. Decarboxylative Borylation of Aliphatic Esters under Visible-Light Photoredox Conditions. *Org Lett* **2017**, *19* (10), 2770-2773. DOI: 10.1021/acs.orglett.7b01181 From NLM.
(26) Johnston, C. P.; Smith, R. T.; Allmendinger, S.; MacMillan, D. W. Metallaphotoredox-catalysed sp(3)-sp(3) cross-coupling of carboxylic acids with alkyl halides. *Nature* **2016**, *536* (7616), 322-325. DOI: 10.1038/nature19056 From NLM.
(27) Qin, T.; Malins, L. R.; Edwards, J. T.; Merchant, R. R.; Novak, A. J.; Zhong, J. Z.; Mills, R. B.; Yan, M.; Yuan, C.; Eastgate, M. D.; et al. Nickel-Catalyzed Barton Decarboxylation and Giese Reactions: A Practical Take on Classic Transforms. *Angew Chem Int Ed Engl* **2017**, *56* (1), 260-265. DOI: 10.1002/anie.201609662 From NLM.
(28) Zhong, Q.; He, M.; Guo, Y.; Zhang, Y. Mass Diffusion Coefficients of Oxygenated Fuel Additives in Diesel Oil and in Heptane at T = (276 to 333) K. *Journal of Chemical & Engineering Data* **2009**, *54* (6), 1666-1671. DOI: 10.1021/je800747v.
(29) Ripenko, V.; Vysochyn, D.; Klymov, I.; Zhersh, S.; Mykhailiuk, P. K. Large-Scale Synthesis and Modifications of Bicyclo[1.1.1]pentane-1,3-dicarboxylic Acid (BCP). *The Journal of Organic Chemistry* **2021**, *86* (20), 14061-14068. DOI: 10.1021/acs.joc.1c00977.